International Journal of Coal Geology 84 (2010) 293–300

Contents lists available at ScienceDirect

International Journal of Coal Geology

journal homepage: www.elsevier.com/locate/ijcoalgeo

Reactivity to CO_2 of chars prepared in O_2/N_2 and O_2/CO_2 mixtures for pulverized coal injection (PCI) in blast furnace in relation to char petrographic characteristics

Juliana G. Pohlmann [a,*], Eduardo Osorio [a], Antonio C.F. Vilela [a], Angeles G. Borrego [b]

[a] Iron and Steelmaking Laboratory, UFRGS, P.O. Box 15021, 91501-970, Porto Alegre, Brazil
[b] Instituto Nacional del Carbón, CSIC, P.O. Box 73, 33080, Oviedo, Spain

ARTICLE INFO

Article history:
Received 26 February 2010
Received in revised form 16 October 2010
Accepted 18 October 2010
Available online 29 October 2010

Keywords:
Blast furnace
Coal char
Optical texture
Specific surface
Combustion
Oxy-fuel
Reactivity

ABSTRACT

Pulverized coal injection (PCI) is employed in blast furnace tuyeres in order to increase the injection rate without increasing the amount of unburned char inside the stack. When coal is injected with air in the region of tuyeres, the resolidified char will burn in an atmosphere with progressively lower oxygen content and higher CO_2 concentration. In this study, an experimental approach comprising refiring has been followed to separate the combustion process into two distinct devolatilization and combustion steps. A drop tube furnace (DTF) operating at 1300 °C in an atmosphere with low oxygen concentration was used to simulate devolatilization and then the char was refired into DTF at the same temperature under two different atmospheres O_2/N_2 (typical combustion) and O_2/CO_2 (oxy-combustion) with the same oxygen concentration. Coal injection was also performed under a higher oxygen concentration in both typical combustion and oxy-combustion atmospheres. The fuels tested comprised a petroleum coke and coals ranging in rank from high to low volatile bituminous, currently used for PCI injection. Specific surface areas, reactivity to CO_2 and char petrography have been used to chars characterization. The morphology and appearance of the chars generated under oxy-fuel (O_2/CO_2) and conventional combustion (O_2/N_2) conditions with similar amount of oxygen were similar for each parent coal. Vitrinite-rich particles generated cenospheres with anisotropic optical texture increasing in size with increasing coal rank, whereas inertinite yielded a variety of morphologies and optical textures. The apparent reactivity to CO_2 measured at high temperature (1000 °C) tended to increase with burnout reflecting the operation under a regime controlled by internal diffusion in which surface area also increased. This may have a significant effect in the reactivity to CO_2 of the chars inside the stack of the blast furnace, even under oxygen lean atmosphere.

1. Introduction

Pulverized coal injection (PCI) is used in blast furnace tuyeres in order to reduce the amount of coke required to provide energy and reducing gases for blast furnace operation. In high rates of PCI, due to extremely short residence time available for char combustion in blast furnace, unburned char will be carried from combustion zone to the stack and will compete with coke for CO_2 (Kawakami and Yamaguchi, 2000). Excessive amount of unburned material leads to problems in the furnace permeability, decreasing productivity (Babich et al., 2008). Nevertheless, the high rate of PCI is desirable to reduce coke utilization and pig iron costs (Deno and Okuno, 2000). Then, an increase in the injection rate must be related to higher combustion efficiency, avoiding increase unburned char too. Coal ranging from high to low rank, different injection lances designs, different blast conditions (flame temperature and stoichiometry oxygen ratio) and injection of other fuels have been studied in a way to improve combustion conditions (Ariyama, 2000; Gill et al., 2008; Yamaguchi et al., 1992).

There is international concern about substantial decrease in greenhouse gases emissions to the atmosphere. Increasing combustion efficiency and consumption of unburned char via reaction with carbon dioxide in the blast furnace stack become important since it could lead to a decrease in fuel rate, increasing blast furnace productivity and releasing less CO_2 to atmosphere. This way, the optimization of PCI has also been turned to the decrease in environmental impact caused by ironmaking industries.

The conditions prevailing in the tuyeres of blast furnace are very difficult to reproduce at laboratory scale and different devices have been used to achieve high temperatures, high heating rate, some pressure and short residence time such as horizontal ovens (Vamvuka et al., 1996), a shock wave reactor (Gudenau et al., 2002), a wire mesh reactor (Pipatmanomai et al., 2003) and drop tube furnaces (Borrego

* Corresponding author. Federal University of Rio Grande do Sul, Iron and Steelmaking Laboratory–DEMET/PPGEM, Bento Gonçalves Avenue, 9500, P.O. Box 15021, 91501-970 Porto Alegre, RS, Brazil. Tel.: +55 5133087074; fax: +55 5133087116.
E-mail addresses: juliana.pohlmann@ufrgs.br (J.G. Pohlmann), eosorio@ufrgs.br (E. Osorio), vilela@ufrgs.br (A.C.F. Vilela), angeles@incar.csic.es (A.G. Borrego).

0166-5162 © 2010 Elsevier B.V. Open access under the Elsevier OA license.
doi:10.1016/j.coal.2010.10.008

et al., 2008; Lu et al., 2002; Wall et al., 2002). None of these devices satisfactorily reproduce the conditions prevailing at industrial scale but reasonably approach to some of the variables to which particles are submitted. In the case of the atmospheric drop tube furnace that was used in this study the temperature is lower and the residence time larger than that expected in the tuyeres but still particles are submitted to fast devolatilization, followed by the combustion of the re-solidified char under dynamic conditions. The experimental approach followed consisting on direct combustion and oxy-combustion of coal, followed by re-firing experiments under both combustion and oxy-combustion atmospheres to approach to the environment of the coal particles in the blast furnace has been followed in a previous study (Borrego et al., 2008). This work complements the previous one with further petrographic information and data on specific surface area and high temperature reactivity to CO_2, which allows an in-depth discussion on the evolution of char reactivity, both apparent and intrinsic, during combustion. This approach could be also useful if technologies of CO_2 capture are to be implemented in steel industry (Hu et al., 2006). The high CO_2 partial pressure in blast furnace gases makes technologies such as separating membranes or amine scrubbing appropriated for CO_2 separation (Ariyama et al., 2009), but other options such as oxy-fuel PCI injection may also be possible. In the latter, coal would be injected in the tuyeres with a mixture of oxygen and recycled CO_2, thus avoiding N_2 and minimizing the step of concentrating CO_2 in the flue gases.

2. Experimental

The selected fuels are typical PCI coals that are used worldwide and a low sulfur (0.9%) petroleum coke (PC) from Brazil. The coals are in increasing rank order: Guasare (GU) from Venezuela, and Black Water (BW) and Jellinbah (JB) from Australia. The samples were ground and sieved to 36–75 μm, which are within the largest range of pulverized particle and therefore comprise the harder to burn fraction of each coal. Proximate, ultimate and petrographic analyses were performed according to the appropriate ISO standards. The ISO standards were followed to perform proximate (ISO 17246:2010), ultimate (ISO 17247, 2005) and petrographic analyses both vitrinite reflectance (ISO 7404-5:2009) and maceral composition (ISO 7404-3:2009) of the parent coals.

Coal chars were prepared at 1300 °C temperature in a drop tube furnace as described elsewhere (Borrego and Alvarez, 2007). The flow rate was 900 l h^{-1} for the body of the reactor and 300 l h^{-1} for the feeder, which entrained the particles at a rate of 1 g min^{-1} through a water-cooled injection probe placed on at the top. The estimated residence time of the particles in the reactor was around 200 ms and the chars left the reactor through a collection probe, to which an extra nitrogen flow was added to quench the reaction and improve collection efficiency in the cyclone. The desired gas composition was achieved with blends of air and N_2 for the O_2/N_2 series and blends of O_2 and CO_2 for the O_2/CO_2 series. The gas compositions and sequence of experiments used in this study are summarized in Fig. 1. The rationale for this approach was described in detail by Borrego et al. (2008) and will be only briefly outlined below. The injection of coal in a low oxygen atmosphere (2.5% O_2 in N_2) produces devolatilization without significant combustion similar to the conditions in the injection lance. Injection of coal in 10% O_2 accompanied by either N_2 or CO_2 guarantees burnouts in the range of 60%–90% (Borrego et al., 2008) under both conventional combustion and oxy-combustion atmospheres. The 2.5% O_2 chars were again fed into the reactor using 5% O_2 in both N_2 and CO_2 to obtain a result for char combustion at high temperature after the emission of volatiles has ceased. An atmosphere rich in CO_2 was selected to represent the enrichment in CO_2 occurring higher up the blast furnace. The chars obtained under O_2/CO_2 atmospheres will be referred to as oxy-chars as opposed to the term "char," which will be restricted to chars obtained under O_2/N_2 atmospheres. Coal GU could not be used in all the experiments because of the lack of samples.

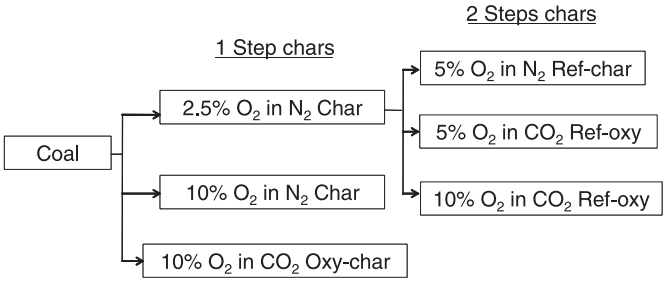

Fig. 1. Scheme of the experimental approach followed for char preparation in this study.

Burnout was calculated using the following ash tracer expression (Carpenter and Skorupska, 1993):

$$Burnout\ (\%) = \left[1-\left(\frac{Ash_{coal.}}{100-Ash_{coal.}}\right)\left(\frac{100-Ash_{char-comb.}}{Ash_{char-comb.}}\right)\right]\times 100$$

assuming that ashes did not suffer any further transformation in the reactor than that undergone during the ISO ashing test (ISO 17246:2010).

The char samples were embedded in polyester resin mixing a small amount of resin with char particles and extending a thin bed on a mould of 0.5 × 0.5 cm. Once the mixture is hard the sample is re-embedded in resin to facilitate polishing. Thick abrasive papers are avoided during polishing to minimize the damage of the fragile char walls. Samples were examined under incident polarized light using 1 lambda retarder plate.

Two widely used methods of determining the pore surface area of carbon from gas adsorption isotherms were applied in this study to selected char samples, using CO_2 at 0 °C and N_2 at −196 °C as adsorptives. The equipment used was a Micromeritics ASAP 2020. Chars were outgassed under vacuum prior to gas adsorption experiments in order to eliminate moisture or condensed volatiles, which could prevent the adsorbate accessibility. The heating rate used was 5 °C min^{-1} with holding temperatures of 90 °C (1 h) and 350 °C (4 h). This temperature is well below the char preparation temperature and is not expected to modify the structure of the char. The Brunauer–Emmett–Teller (BET) theory was applied to the N_2 adsorption data to obtain the surface area (Brunauer, Emmett and Teller, 1938). CO_2 adsorption isotherms were performed in one sample of each series up to a pressure of 0.035 torr, and the Dubinin–Radushkevich (D–R) equation was applied to the adsorption data (Dubinin and Radushkevich, 1947). These two methods can be regarded as complementary, given the difficulties of CO_2 to fill large micropores and the slow diffusion of N_2 in the small micropores (Jagiello and Thommes, 2004). Only one sample of each series was analyzed for CO_2 adsorption because previous studies have shown negligible variation of CO_2 surface area along combustion in medium rank coals (Alvarez and Borrego, 2007; Borrego and Alvarez, 2007). As some of the samples contained large amounts of mineral matter and the adsorption capacity of chars is essentially associated to the organic fraction (Maroto-Valer et al., 2001), the surface area data are expressed on an ash-free-basis. Although this is only a rough approach it allows us to compare the surface area of chars at different burnouts as the BET surface area of mineral fraction of fly-ashes vary within a narrow interval and is very low (0.7–0.8 m^2g^{-1} according to Külaots et al., 2004). Therefore the actual surface area of the organic fraction could be expected to be around 1–2 % lower than the reported values, which still permits to establish differences between the various chars of this study. Unfortunately, independent determination of ash surface area was not possible due to the large amount of

material required for the assay when the adsorption capacity of the material is very low.

The reactivity of chars to CO_2 at high temperature has been used to resemble the conditions that char particles are seeing once they leave the injection zone and ascend in the blast furnace. In this region char particles compete with coke and therefore a similar test to that for assessing coke reactivity (Patrick et al., 1980) has been used. The reactivity of the chars to CO_2 was evaluated by thermogravimetric analysis in a STA 409 PC Luxx apparatus. A small quantity of char (8 mg) was homogeneously spread on the bottom of the crucible and heated up to 1000 °C under nitrogen flow (60 ml min^{-1}) at a heating rate of 30 °C mim^{-1}. Immediately the reactant gas was changed to CO_2 at the same flow rate and the temperature was maintained until weight stabilization. The weights were corrected for buoyancy effects. Conversion (X) and apparent reactivity at 50% of conversion ($R_{50\%}$) on an ash-free basis were calculated using the following expressions:

$$X = \left(\frac{m_0 - m}{m_0}\right) \times 100 \qquad R_{50\%} = \frac{1}{m_0}\left(\frac{dm}{dt}\right)_{50\%}$$

with m_0 being the initial sample weight ash-free and m being the instantaneous sample weight. The reactivities so obtained will be compared to those isothermally recorded in air at 550 °C under similar flow gas conditions and reported previously (Borrego et al., 2008). An estimate of the intrinsic reactivity of the carbonaceous material, once the effect of surface area has been discounted, can be obtained dividing the apparent reactivity by the surface area.

3. Results and discussion

3.1. Coal characteristics

The coals in Table 1 have ash contents below 10% as typically specified for coals to be used in PCI and relatively low sulfur content (<1.1%). The volatile matter content, vitrinite reflectance and chemical analyses (C, H, and O contents) vary as expected for the rank of the coals ranging from high volatile bituminous (ASTM D388-05) or Medium Rank C (ISO 11760: 2005) in the case of coal GU to low volatile bituminous or Medium Rank A in the case of coal JB. The three coals have moderate inertinite content in the range 20–35 vol.% and low liptinite content. The petroleum coke (PC) has volatile matter content around 12%, which is within the interval corresponding to semi-anthracite volatile matter content (8–14% volatile matter) according with ASTM D0388 (2005). PC has a very low ash and sulphur contents, the latter unusual in petroleum coke which makes this particular coke especially attractive for pulverized coal injection.

3.2. Oxy-combustion versus conventional combustion

The burnout of the various coals was closely related to their rank and decreased from GU to JB (Borrego et al., 2008) (Fig. 1). This is an expected result commonly reported in the literature (Alvarez et al., 1998; Bend et al., 1992; Cloke et al., 1997). The increments observed between combustion taking place under highly sub-stoichiometric conditions (2.5%O_2 in N_2) and under slightly over-stoichiometric (10% oxygen in one step or refired chars to 5%O_2) conditions were also rank dependant (Borrego et al., 2008). The smallest increment (around 47%) occurred for coal GU, it was intermediate for coal BW (57%), and the largest for the highest rank coal JB (75%). This gives an indication of the reactivity of the coals. The burnouts of the chars prepared with either 10% O_2 in one step or 5%O_2 after refiring were similar regardless the accompanying gas (CO_2 or N_2). Contradictory results have been achieved in recent studies when combustibility of coals under conventional combustion (O_2/N_2) and oxy-combustion conditions (O_2/CO_2) have been compared (Buhre et al., 2005). Some studies report lower burnouts in oxy-combustion atmosphere that have been attributed to the lower specific heat of CO_2 (Liu et al., 2005), which also lowers the particle peak temperature (Bejarano and Levendis, 2008; Schiemann et al., 2009). Some others have reported similar or even higher burnouts under oxy-fuel atmosphere (Borrego et al., 2008; Borrego and Martín, 2010; Rathnam et al., 2009), which can be attributed to the reaction of char to CO_2 at high temperatures. In addition, the burnouts of the chars prepared with 2.5% O_2 and refired at an O_2 concentration of 5% in both N_2 and CO_2 were similar to their counterparts obtained directly from coal at an O_2 concentration of 10%. This gave us the opportunity to compare the performance of coals in one step and two step combustion (first devolatilization and then consumption of the char).

Table 1
Proximate, ultimate and petrographic analyses of the individual fuels*.

Sample	Ash	S_t	VM	C	H	N	O	R_r	V	L	I
	% db		% daf					%	% vol. mmf		
GU	6.9	1.1	42.5	82.2	5.1	1.7	9.9	0.63	77.2	2.4	20.4
BW	9.5	0.6	29.3	83.4	4.3	2.0	10.6	1.02	61.8	2.8	35.4
JB	9.8	0.6	17.6	87.2	3.8	1.9	5.6	1.56	69.3	-	30.7
PC	0.1	0.9	11.7	91.3	3.9	1.2	2.7				

S_t = total sulphur; VM = volatile matter; R_r = random vitrinite reflectance; V = vitrinite; L = liptinite; I = inertinite; db = dry basis; daf = dry-ash-free basis; vol = volume; mmf = mineral matter-free.

3.3. Char petrography

The appearance of the chars under the incident light optical microscope is described below. The high volatile bituminous (hvb) coal GU yielded material having mostly isotropic appearance under relatively low magnification (Fig. 2b), but examination of the vitrinite-derived char walls at high magnification revealed incipient anisotropy development (Fig. 2a). The vitrinite-derived particles had cenospheric shape with relatively thick walls with smaller bubbles within the walls as typically expected for a high volatile bituminous coal (Alonso et al., 2001). Extensively burned chars (85% burnout) had similar optical texture and even thicker walls, although many particles were fragmented. The medium volatile bituminous (mvb) coal BW yielded mainly anisotropic char material. Vitrinite generated hollow particles with a small mosaic-optical texture (Fig. 2c), whereas inertinite generated either massive unfused isotropic particles or anisotropic particles with a network structure (Fig. 2d). The optical texture of vitrinite-derived particles in the chars from the low volatile bituminous (lvb) coal JB was larger (Fig. 2e), indicating an improved ordering compared to the vitrinite of coal BW (Fig. 2c) and the occurrence of a plastic stage during devolatilization when aromatic units had the time to grow and stack. The inertinite-derived material in JB char exhibited heterogeneous structure and optical texture (Fig. 2f) as in the case of coal char BW. The petroleum coke yielded two types of particles, one of which yielded massive particles, with large size optical texture typical of petroleum coke (Fig. 3a, b and d). These particles typically exhibited fissures surrounding the anisotropic domains through which volatiles had evolved and through which combustion can proceed. The other type of particles had developed abundant porosity and either well-formed network (Fig. 3a and c) and in some cases balloon-like structures (Milenkova et al., 2003). The chars from high burnout runs had very few completely intact particles but abundant fragments derived from the collapse of the particles.

3.4. Specific surface area

A previous study of char textural properties showed that the presence of variable amount of oxygen in the combustion atmosphere hardly affected the micropore surface area (S_{CO2}), which is mainly due

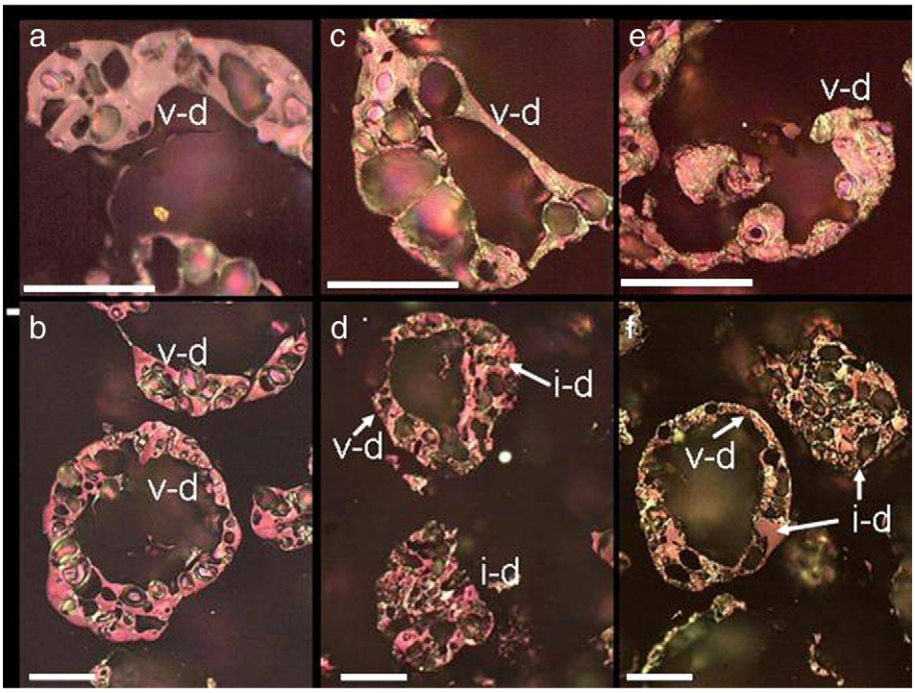

Fig. 2. Appearance of the coal chars from the hvb coal GU (a) and (b), the mvb coal BW (c) and (d) and the lvb coal JB (e) and (f). v-d and i-d mean vitrinite- and inertinite-derived, respectively. Images taken with incident polarized light and 1 lambda retarder plate. Scale bar: 25 microns.

to the structural porosity left by the re-organization of the carbonaceous material during resolidification (Feng and Bhatia, 2003), but strongly affected the mesopore (S_{BET}) surface area (Alvarez and Borrego, 2007). This was so for high volatile bituminous coals generating disordered isotropic material typically resulting in large micropore surface areas and for low volatile bituminous coals passing through a plastic stage and generating chars with low microporosity. The micropore surface area (S_{CO2}) for each series of coal chars was similar for the three coal chars (around 150 $m^2\ g^{-1}$). The S_{CO2} value for JB char (150 $m^2\ g^{-1}$) is higher than expected for a low volatile bituminous coal rank (Alonso et al., 2001; Borrego and Alvarez, 2007). The described behavior regarding re-organization of the carbonaceous material during re-solidification would only affect the vitrinite, whereas around 30% of the coal would have lower plasticity resulting in less annihilation of microporous surface area. The high inertinite content of coal BW would also explain the small difference in S_{CO2} of the two series of chars (S_{CO2} for BW series was 161 $m^2\ g^{-1}$), because inertinite-derived chars have lower S_{CO2} than vitrinite-derived chars for high volatile bituminous-medium volatile bituminous coals, but higher S_{CO2} than low volatile bituminous vitrinite-derived chars (Alonso et al., 2001). In the case of chars GU no satisfactory explanation could be found for such a low S_{CO2} (S_{CO2} for GU series was 158 $m^2\ g^{-1}$) which is around half of what it could be expected for high volatile bituminous chars (Alonso et al., 2001; Borrego and Alvarez, 2007). A tentative explanation could be found in the low ash fusion temperatures of this coal (Bagatini et al., 2009), which may have caused blockage of porosity and a decrease in S_{CO2}. The PC char had a very low S_{CO2} (21 $m^2\ g^{-1}$), which is consistent with the highly ordered carbonaceous structure of petroleum coke.

The BET surface area is able to account for mesoporosity and not only narrow micropores. The evolution of S_{BET} for the three series of chars is shown in Fig. 4 referred to burnout. The combustion of particles in the size interval used in this study (36–75 microns) at high temperatures can be considered to operate in an external to internal diffusion controlled regime (regime III–II) in which combustion proceeds through widening of micropores (Alvarez and Borrego, 2007; Gale et al., 1995). Although both the S_{BET} and S_{CO2} of the three chars obtained under low oxygen concentration were rather similar,

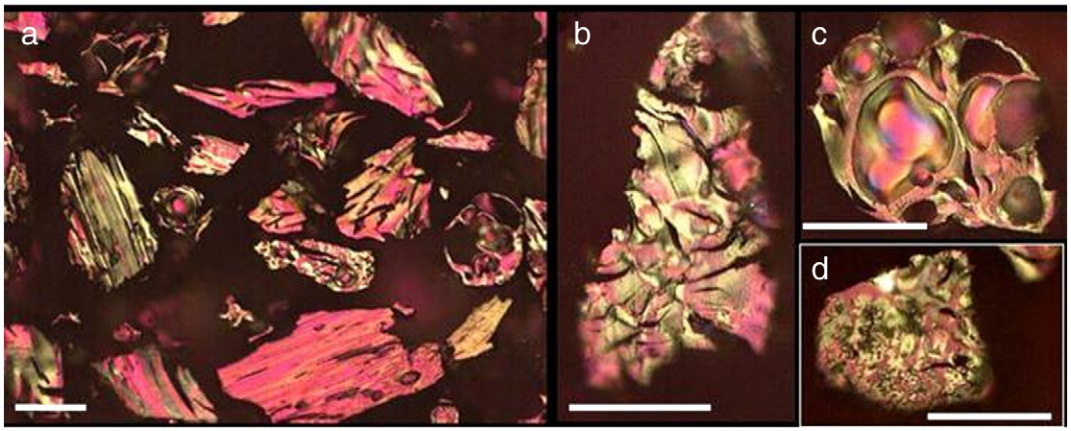

Fig. 3. Appearance of the petroleum coal chars (PC) generated in the drop tube reactor with low oxygen concentration showing massive and porous structure. Images taken with incident polarized light and 1 lambda retarder plate. Scale bar: 25 microns.

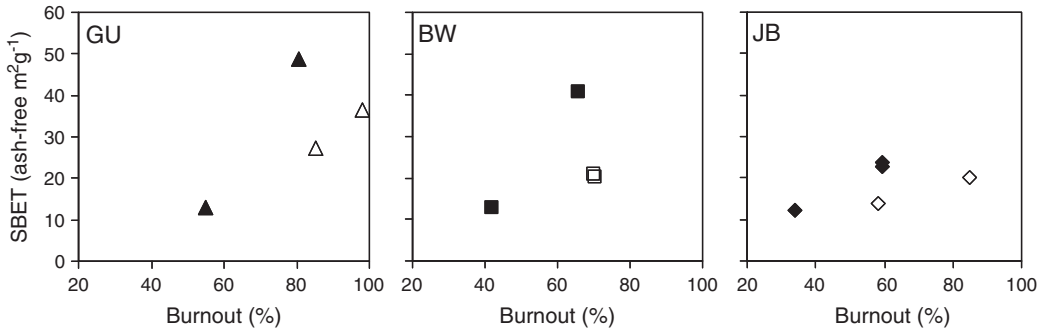

Fig. 4. Evolution of surface area with burnout for the various coal chars. hvb coal GU (a), mvb coal BW (b) and lvb coal JB (c). Solid symbols: 1 step combustion, and void symbols: refired chars.

the evolution of S_{BET} in Fig. 4 shows higher increase, the lower the rank of the coal, indicating important differences in the structure of the chars. The chars with a more disordered structure (essentially isotropic chars) underwent the largest increase in S_{BET}, whereas the chars from the highest rank coal, in which predominant porosity is expected to be slit-shaped associated to the ordered anisotropic domains experienced a lower increase in S_{BET}. In comparison with combustion in 1 step, in which oxygen is present in the devolatilizing atmosphere, the combustion in 2 steps, after refiring, resulted for the three chars in lower increments in S_{BET} (Fig. 4). In the cases in which pairs of O_2/N_2 and O_2/CO_2 chars were available the S_{BET} values were close to each other.

3.5. Char reactivity

The apparent reactivity of the 1 step chars to CO_2 measured at 1000 °C in a thermobalance was higher, the lower the rank of the parent coal, except for the 2.5% O_2 char of coal GU. Apparent reactivities were the lowest for the PC, which had the lowest volatile matter content of the studied fuels (Fig. 5a). Similar apparent reactivities were obtained for the highly combusted and poorly combusted chars except in the case of 2.5% O_2 GU char, which had an unexpectedly lower reactivity. A similar result was found for the apparent reactivity of GU chars to air (Borrego et al., 2008). Once the CO_2 reactivities were corrected for surface area the intrinsic reactivity of the material became apparent (Fig. 5b). In this case the intrinsic reactivities of the highly combusted chars were lower than those of the devolatilized chars, an expected result considering the deactivation of residual material during combustion (Hurt and Gibbins, 1995). The differences between the intrinsic reactivities of the poorly combusted chars were larger than for the 10% O_2 chars. The reactivity of the 10% oxygen chars compared to the 2.5% chars did not follow a consistent trend. As seen in Fig. 5b the intrinsic reactivity of the poorly combusted GU char was very low. No satisfactory explanation for this behavior based on the char structure or chemical composition of the parent coal can be advanced at this stage.

Fig. 6 shows the evolution of reactivity to CO_2 as a function of burnout for the three coal chars. The burnout determination of PC had very low reliability due to the low ash content of petroleum coke and it was not calculated. For the three coal chars the increase in burnout resulted in an increase in apparent reactivity to CO_2. This increase has to be essentially due to the increase in S_{BET} (Fig. 4), because in GU the intrinsic reactivity was similar during the course of combustion and in BW the intrinsic reactivity decreased with burnout as shown in the graphs of Fig. 6 (bottom). The dispersion of values was very large in the case of JB in which low reactivities are combined with low surface areas. The drop in intrinsic reactivity of extensively burned chars is essentially due to the consumption of the most reactive material in previous steps and to the deactivation occurring in the combustors (Hurt and Gibbins, 1995).

Fig. 7 shows the apparent reactivity of the oxy-char versus the apparent reactivity of the equivalent char obtained under similar oxygen concentration. This is shown for the apparent reactivities to CO_2 measured at 1000 °C (Fig. 7a) and for the apparent reactivity to air measured at 550 °C (Borrego et al., 2008; Fig. 7b). In the case of both reacting gases, the apparent reactivities of the 1 step oxy-combustion and combustion chars were very similar. In the case of the refired chars only the oxy-char from the hvb coal (GU) deviated significantly towards higher apparent reactivities compared with the reactivity of the O_2/N_2 equivalent char. This deviation occurred for both the reactivity measured at low temperature in air and at high temperature in CO_2. It must be mentioned that these results corresponded to extensively burned chars (over 98%) and therefore any determination of reactivity of the organic matter might be subjected to higher analytical errors. Indeed, no determination of S_{BET} could be performed on these samples, which could have assisted in

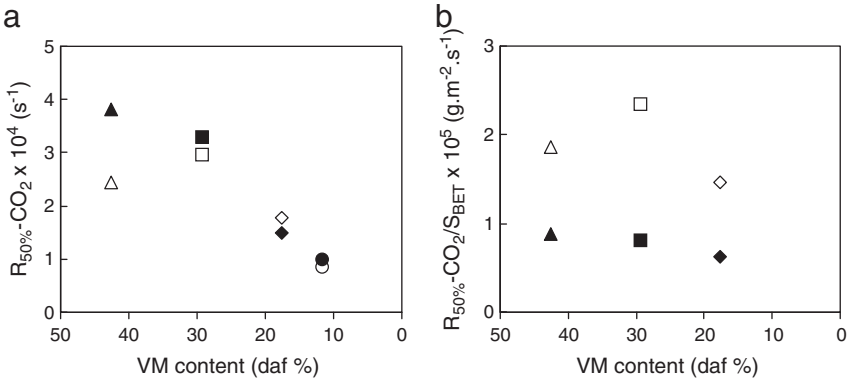

Fig. 5. Reactivity to CO_2 measured at 1000 °C of the chars as a function of the volatile matter content of the parent coal. a) Apparent reactivity. b) Reactivity corrected for surface area (S_{BET}). Void symbols = chars obtained under 2.5%O_2 in N_2 and solid symbols = chars obtained under 10%O_2 in N_2. ▲ = GU; ■ = BW; ◆ = JB; ● = PC.

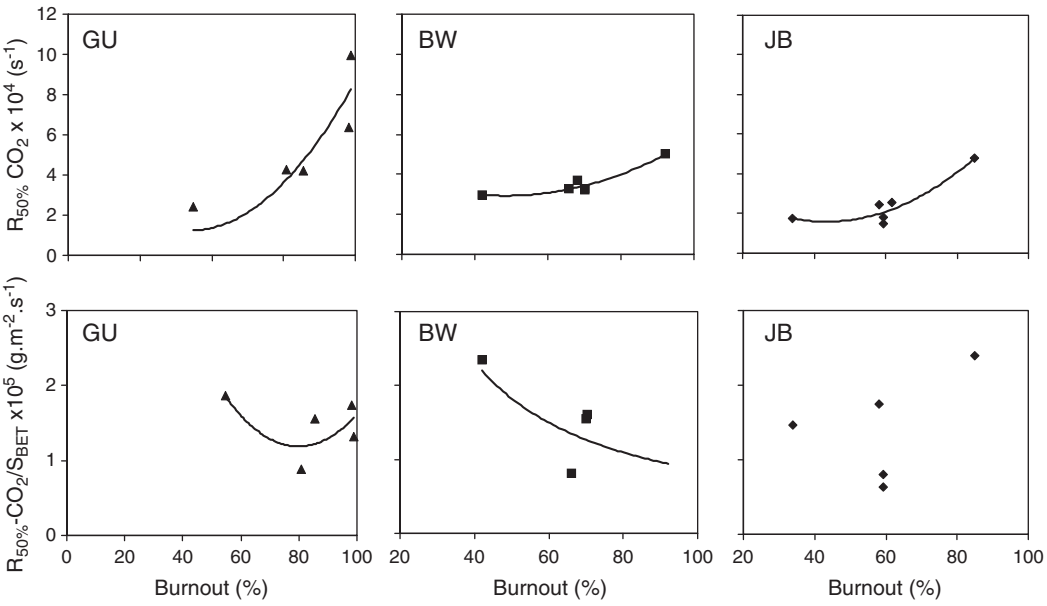

Fig. 6. Top: apparent reactivity to CO_2 of the coal chars as a function of coal burnout. Bottom: intrinsic reactivity corrected for S_{BET} of the coal chars as a function of coal burnout.

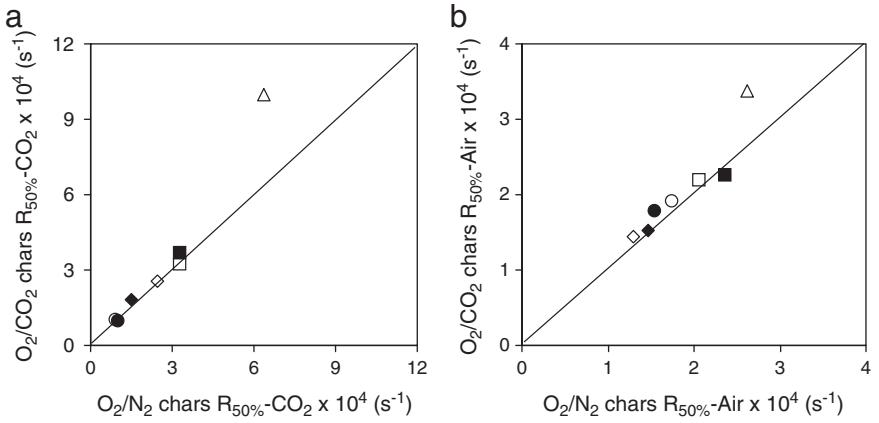

Fig. 7. Conventional combustion (O_2/N_2) versus oxy-combustion under similar oxygen concentrations. a) Reactivity to CO_2 measured at 1000 °C; b) Reactivity to air measured at 550 °C (data from Borrego et al., 2008). Solid symbols = 1step combustion; void symbols = 2 step combustion (refired); ▲ = GU; ■ = BW; ◆ = JB; ● = PC.

the explanation of the result. Similar or higher reactivities obtained to all the samples produced in oxy-combustion conditions indicate, at least, that chars formed under conventional and oxy-fuel conditions at the same oxygen content could not have significant differences when reacted with CO_2 in the blast furnace stack.

Fig. 8 shows burnout versus both the apparent reactivity measured in air at low temperature and the apparent reactivity measured at 1000 °C in CO_2. For the three coal chars a clear trend was observed for the low temperature reactivity to slightly decrease during the course of burnout and the high temperature reactivity to significantly increase with burnout. At the low temperature, the kinetic control of the reaction is ensured and the reacting gas can reach the narrowest porosity (S_{CO2}), which is not expected to significantly change during the course of burnout (Borrego and Alvarez, 2007). On the contrary, the internal diffusion may play a significant role in the reactivity at high temperatures. High temperature reactivity increased for the three coal chars

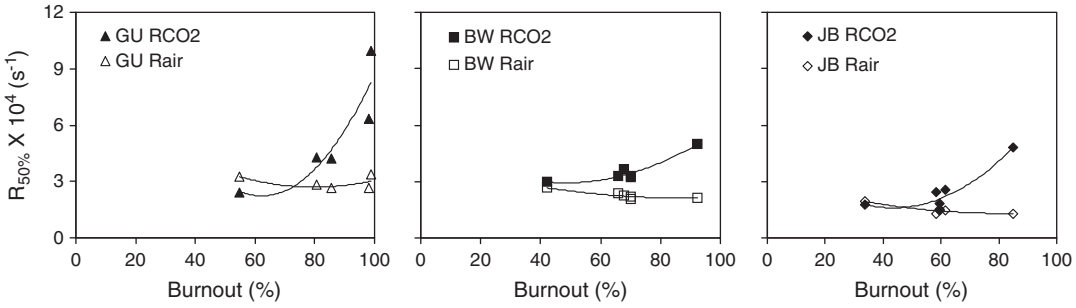

Fig. 8. Evolution of apparent reactivity to CO_2 at high temperature and apparent reactivity to air at low temperature with char burnout.

with burnout, whereas the intrinsic reactivity decreased (Fig. 6). This is coincident with the increase in S_{BET} observed with burnout Fig. 4). The increase in S_{BET} which reflects an increase in wide micro- and mesoporosity would facilitate the diffusion of the gas to the reacting surface then increasing the reactivity. This phenomenon which is observed under the controlled conditions of the thermobalance is expected to be even more important at the higher temperatures occurring in the blast furnace. Under these conditions the higher S_{BET} achieved when particles are devolatilized in the presence of oxygen would favor their combustion in the blast furnace.

The relatively narrow range of reactivities obtained for the various coal chars at low and high temperatures and the positive evolution of reactivity with burnout indicate that the char tested have similar chances to be burn to completion in the blast furnace stack. Therefore parameters such as volatile matter, ash and sulfur contents obtained from proximate and ultimate analysis can be used to select the best coals for PCI.

4. Conclusions

- The morphology and appearance of the chars generated under oxy-fuel (O_2/CO_2) and conventional combustion (O_2/N_2) conditions with similar amount of oxygen were virtually indistinguishable through the optical microscope. Vitrinite-rich particles generated cenospheres with incipient anisotropic optical texture in the high volatile bituminous coal, small anisotropic domains in the medium volatile bituminous coal and well-developed anisotropic domains in the low volatile bituminous coal. Inertinite behaved in a variety of manners yielding massive and porous particles with isotropic and anisotropic optical texture. The optical texture in inertinite-derived material was mainly isotropic in the high volatile bituminous coal and mostly anisotropic in the medium and low volatile bituminous coals. The chars prepared by refiring and having a similar burnout than those from single step combustion were also rather similar in appearance.
- The apparent reactivity to CO_2 measured at high temperatures (1000 °C) tended to increase with burnout reflecting the operation under a regime controlled by internal diffusion. This increase was associated to an increase in surface area measured by N_2 adsorption and BET model (S_{BET}). The apparent reactivity to air measured at low temperature (550 °C) reflected a kinetically controlled regime in which the reacting gas had time for diffusion throughout the porosity reaching the narrowest porosity. The combustion pattern would favor the combustibility of particles which devolatilized in the presence of moderate oxygen concentration in the blast furnace. These particles exhibited larger surface areas (S_{BET}) than 2 step chars of similar burnout (first step = devolatilization; second step = combustion), and would burn at faster rates under diffusion-controlled conditions.
- The reactivity performance and the microscopic appearance of the chars obtained under typical combustion and oxy-combustion atmospheres, simulating recycled CO_2 injection in the blast furnace tuyeres, was very similar. This would indicate that chars formed under conventional and oxy-fuel conditions at the same oxygen content would not differ significantly when reacted in the blast furnace stack.

Acknowledgements

The Brazilian team thanks CNPq for the financial support. Financial support for char preparation and analysis from MICINN (Spain) through Project PSE 2-2005 is gratefully acknowledged. This work was possible thanks to a bilateral co-operation project CSIC-CNPq (2005BR00054). D. Alvarez of INCAR–CSIC is thanked for his assistance and advice for the char preparation.

References

Alonso, M.J.G., Borrego, A.G., Alvarez, D., Parra, J.B., Menéndez, R., 2001. Influence of pyrolysis temperature on char optical texture and reactivity. J. Anal. Appl. Pyrol. 58, 887–909.
Alvarez, D., Borrego, A.G., 2007. The evolution of char surface area along pulverized coal combustion. Energy Fuels 21, 1085–1091.
Alvarez, D., Borrego, A.G., Menendez, R., Bailey, J., 1998. An unexpected trend in the combustion behavior of hvBb coals as shown by the study of their chars. Energy Fuels 12, 849–855.
Ariyama, T., 123-132, 2000. Advanced injection lances for high rate PCI. In: Advanced pulverized coal injection technology and blast furnace operation, 1. ed. Pergamon–Elsevier Science, Oxford, UK, pp. 123–132.
Ariyama, T., Ueda, S., Natsui, S., 2009. Current technology and future aspect on CO2 mitigation in Japanese steel industry. In.: Int. Congr. Sc. Technol. Ironmaking, 5, 2009. Proceedings… Shangai, 55–69.
ASTM Standard D0388, 2005. Standard Classification of Coals by Rank. ASTM International, West Conshohocken, PA. doi:10.1520/D0388-05. www.astm.org.
Babich, A., Senk, D., Gudenau, H.W., Mavrommantis, K.Th., 2008. Ironmaking, first ed. RWTH Aachen University, Aachen. 402 p.
Bagatini, M.C., Ghiggi, M.L.F., Osorio, E., Vilela, A.C.F., Defendi, G., Cruz, R., 2009. Behavior of coal ashes for pulverised coal injection at high temperatures in relation to their chemical and mineralogical composition: Experimental and computational analysis. Ironmaking Steelmaking 36 (8), 583–589.
Bejarano, P.A., Levendis, Y.A., 2008. Single-coal-particle combustion in O_2/N_2 and O_2/CO_2 environment. Combust. Flame 153, 270–287.
Bend, S.L., Edwards, I.A.S., Marsh, H., 1992. The influence of rank upon char morphology and combustion. Fuel 71, 493–501.
Brunauer, S., Emmett, P., Teller, E.J., 1938. Adsorption of gases in multimolecular layers. Am. Chem. Soc. 60, 309–315.
Borrego, A., Alvarez, D., 2007. Comparison of chars obtained under oxy-fuel and conventional pulverized coal combustion atmospheres. Energy Fuels 21, 3171–3179.
Borrego, A.G., Osorio, E., Casal, M.D., Vilela, A.C.F., 2008. Coal char combustion under a CO_2-rich atmosphere: Implications for pulverized coal injection in a blast furnace. Fuel Process. Tech. 89 (11), 1017–1024.
Borrego, A.G., Martín, A.J., 2010. Variation in the structure of anthracite at a fast heating rate as determined by its optical properties: An example of oxy-combustion conditions in a drop tube reactor. Int. J. Coal Geol. 81, 4, 301-308. doi:10.1016/j.coal.2009.05.004.
Buhre, B.J.P., Elliot, L.K., Sheng, C.D., Gupta, R.P., Wall, T.F., 2005. Oxy-fuel combustion technology for coal-fired power generation. Progr. Energy Comb. Sci. 31, 283–307.
Carpenter, A., Skorupska, N., 1993. Coal combustion: Analysis and testing: IEA Coal Research, IEACR/64, 97 p.
Cloke, M., Lester, E., Gibb, W., 1997. Characterization of coal with respect to carbon burnout in pf-fired boilers. Fuel 76, 1257–1267.
Deno, T., Okuno, Y., 2000. Introduction—High rate PCI operation in Japan. In: Advanced pulverized coal injection technology and blast furnace operation. 1. ed. Oxford, UK: Pergamon–Elsevier Science, pp. 1-14.
Dubinin, M.M., Radushkevich, L.V., 1947. Equation of the characteristic curve of activated charcoal. Proc. Acad. Sci. URSS 55, 331–335.
Feng, B., Bhatia, S.K., 2003. Variation of the pore structure of coal chars during gasification. Carbon 41, 507–523.
Gale, T.K., Fletcher, T.H., Bartholomew, C.H., 1995. Effects of pyrolysis conditions on internal surface areas and densities of coal chars prepared at high heating rates in reactive and nonreactive atmospheres. Energy Fuels 9, 513–524.
Gill, T., Gupta, S., Sahjawalla, V., 2008. Effect of blending pet-coke on combustion characteristics of PCI coals. In: International Meeting on Ironmaking, 3. 2008, Sao Luiz City, MA, Brazil. Proceeding… Sao Paulo City: Associação Brasileira de Metalurgia e Materiais, 2008, pp. 833-844.
Gudenau, H.W., Senk, D., Fukada, K., Babich, A., Froehling, C., 2002. Coke behaviour in the lower part of the blast furnace with high injection rate. Proceedings of International BF Lower Zone Symposium, Wollongong. pp. 1–12.
Hu, C., Chen, L., Zhang, C., Qi, Y., Win, R., 2006. Emission mitigation of CO_2 in steel industry: Current status and future scenarios. Int. J. Iron and Steel Research 13, 6, 52, 38-42.
Hurt, R.H., Gibbins, J.R., 1995. Residual carbon from pulverized coal-fired boilers. 1: Size distribution and combustion reactivity. Fuel 74, 471–480.
ISO 11760, 2005. Classification of coals. International Organization for Standardization, Geneva, 9 pp.
ISO 7404-3, 2009. Methods for the petrographic analysis of coals—Part 5: Method of determining maceral group composition, International Organization for Standardization, Geneva, 7 pp.
ISO 7404-5, 2009. Methods for the petrographic analysis of coals—Part 5: Method of determining microscopically the reflectance of vitrinite, International Organization for Standardization, Geneva, 14 pp.
ISO 17246:2010. Coal-proximate analysis, International Organization for Standardization, Geneva, 5 pp.
ISO 17247:2005. Coal-ultimate analysis, International Organization for Standardization, Geneva, 4 pp.
Jagiello, J., Thommes, M., 2004. Comparison of DFT characterization methods based on N_2, Ar, CO_2, and H_2o adsorption applied to carbons with various pore size distributions. Carbon 42, 1227–1232.
Kawakami, M., Yamaguchi, K., 2000. Burden properties suitable for high rate PCI. Advanced pulverized coal injection technology and blast furnace operation. Pergamon–Elsevier Science, Oxford, UK, pp. 217–257.
Liu, H., Zailani, R., Gibbs, B.M., 2005. Comparisons of pulverized coal combustion in air and in mixtures of O_2/CO_2. Fuel 84, 833–840.

Lu, L., Sahajwalla, V., Kong, C., McLean, A., 2002. Chemical structure of chars prepared under conditions prevailing in the blast furnace PCI operation. ISIJ Int. 42, 816–825.
Külaots, I., Hurt, R.H., Suuberg, E.M., 2004. Size distribution of unburned carbon in coal fly-ash and its implications. Fuel 83, 223–230.
Maroto-Valer, M.M., Taulbee, D.N., Hower, J.C., 2001. Characterization of differing forms of unburned carbon present in fly ash separated by density gradient centrifugation. Fuel 80, 795–800.
Milenkova, K.S., Borrego, A.G., Álvarez, D., Xiberta, J., Menéndez, R., 2003. Devolatilization behaviour of petroleum coke under pulverised fuel combustion conditions. Fuel 82, 1883–1891.
Patrick, J.W., Sims, M.J., Stacey, A.E., 1980. The relation between the strength and structure of metallurgical coke. J. Phys. D Appl. Phys. 13, 937–951.
Pipatmanomai, S., Paterson, N., Dugwell, D.R., Kandiyoti, R., 2003. Investigation of coal conversion under conditions simulating the raceway of a blast furnace using a pulsed air injection wire-mesh reactor. Energy Fuels 17, 489–497.
Rathnam, R.K., Elliot, L.K., Wall, T.F., Liu, Y., Moghtaderi, B., 2009. Differences in reactivity of pulverized coal in air (O_2/N_2) and oxy-fuel (O_2/CO_2) conditions. Fuel Process. Tech. 90, 797–802.
Schiemann, M., Scherer, V., Wirtz, S., 2009. Optical Coal Particle Temperature measurement under oxy-fuel conditions: Measurement methodology and initial results. Chem. Eng. Tech. 32, 2000–2004.
Vamvuka, D., Schwanekamp, G., Gudenau, H.W., 1996. Combustion of pulverized coal with additives under conditions simulating blast furnace injection. Fuel 75, 1145–1150.
Yamaguchi, K., Ueno, H., Tamura, K., 1992. Maximum injection rate of pulverized coal into blast furnace through tuyeres with consideration of unburnt char. ISIJ Int. 32 (6), 716–724.
Wall, T.F., Liu, G.-S., Wu, H.-W., Roberts, D.G., Benfell, K.E., Gupta, S., et al. , 2002. The effects of pressure on coal reactions during pulverised coal combustion and gasification. Prog. Energ. Comb. Sci. 28, 405–453.